Journal of the Technical University of Gabrovo

https://mc04.manuscriptcentral.com/jtug

INVESTIGATING THE EFFECT OF THE INFILL DENSITY AND GEOMETRY ON SOME MECHANICAL PROPERTIES OF PETG COMPONENTS MANUFACTURED USING FUSED FILAMENT FABRICATION

Nikolay Petrov*

Technical University of Gabrovo, 5300 Gabrovo, Bulgaria

ARTICLE INFO

Article history:
Received 5 June 2025
Accepted 10 July 2025

Keywords:
fused filament fabrication; PETG; infill; tensile properties; flexural properties

http://doi.org/10.62853/LIVX2292

ABSTRACT

In this work the effect of the infill density and geometry on the tensile and flexural properties of polyethylene terephthalate glycol (PETG) samples prepared using fused filament fabrication (FFF) was investigated. The infill density was varied between 15 %, 25 %, and 35 %, and the samples were denoted as T1, T2, and T3, correspondingly. All samples exhibited similar tensile strength with the maximum one being 18.05 MPa of the 35 % infill density sample. The flexural strength of samples T1-T3 was nearly identical meaning the infill density did not have a major effect on it. Based on the performed mechanical tests, the highest infill density was chosen to prepare three more samples where the infill geometry was varied. Three infill geometries were used, namely a triangular one, a honeycomb one, and an octet one, with samples denoted at T4, T5, and T6, accordingly. The results indicated that the highest tensile force of 18.31 MPa was achieved by using a honeycomb infill pattern, however, the octet pattern sample exhibited the highest flexural strength of 32.40 MPa. Samples T5 and T6 also required the highest printing time and raw material input, thus increasing the material cost for production. However, the obtained results emphasize the importance of selecting an appropriate design for the desired application where an optimal choice between cost and functionality should be made.

1. INTRODUCTION

Rapid prototyping is a term that has existed since the 80s as a means to prototype new ideas and designs quickly and efficiently. This was done initially predominantly in the form of small scale designs that would give a comprehensive understanding of the success of the visual and practical aspects of the design in the pre-production stage, which would simplify and quicken the re-design (should one be needed). In recent years, this term has evolved into "additive manufacturing (AM)" referring to the possibility of not just prototyping, but full-scale production of components. Unlike some typical means of manufacturing that rely on subtraction of material, in additive manufacturing the products are made by adding material to them, using a layer-by-layer architecture [1]. This is achieved in various ways, depending on factors such as production time, ease of production, level of automation, deposition accuracy, material choice, and others. Different techniques and systems for AM have been developed up until now, which based on the material used for production are divided into ones suitable for manufacturing polymeric or metallic components [2, 3]. Out of the many 3D printing systems designed for the manufacturing of polymeric components, the most common one is the so-called fused filament fabrication (FFF). It is based on the use of tubular filaments that are heated, melted and applying on the printing surface. The entire process is computer controlled and automated. These types of systems are known for their great accuracy, good layer adhesion, and fast deposition speed [4]. In addition, the cost related to the design and manufacturing of such a system are lower compared to other implementing more complex methods for layer-to-layer deposition.

Polymers have been investigated by scientists since the 19th century. Various theories have been proposed regarding the structures of polymeric materials and how they correspond to their chemical and physical properties. Regardless of the substantial progress in that field, in the early days of the 20th century, particularly with the founding of what is considered to be the first commercially manufactured synthetic polymer – bakelite by Leo Baekeland [5], it was not until the 1930-40s that the structure of polymers began to be properly defined [6]. With the recent, at the time, discoveries in the field the chemical and physical processes involving the manufacturing and modification of polymers a new age of products arose with extreme application in all fields of the human world such as automotive, food and drink industries, drug fabrication, delivery, and storage, fabrics, even in aeronautics. Terms like linear and nonlinear condensation and linear and nonlinear addition polymers began to emerge, which substantially improved the understanding of

* Corresponding author. E-mail: nikolaypetrov44@mail.bg

the type and order of monomeric and functional group bonds. For decades the question regarding quantifying the molecular mass of polymers persisted with different researches providing vastly different results, some of which seemed way too low, and some of which seemed outlandishly large. With the advancement of technology and methods for characterization it became possible to accurately determine the molecular mass of polymers of differing kinds [7, 8]. This is of extreme importance since polymers with high molecular mass have great structural and functional properties. Some considered that high molecular mass also was indicative of high chemical stability, however, those claims were debunked and it was found that molecular mass had little to no effect on the chemical response of polymers [9]. A much more important factor was found to be the bonding of the constituent compounds. The architecture of the polymers is of much greater importance to their properties such as strength, viscosity, chemical reactivity, etc. Structurally three basic types of polymers can be defined – crystalline, semi-crystalline, and amorphous [10, 11]. Crystalline polymers typically possess high strength, especially when a homogeneous orientation of the crystals has been achieved, and better thermal stability, however, also characterize as more brittle and harder to form. Semi-crystalline polymers also have good strength and are more malleable, but their properties are highly dependent on the density and orientation of the crystals. Amorphous polymers typically have lower strength and softening temperatures, however, much higher plasticity and chemical resistance. This is largely due to the isotropic nature of the relationship between structure and properties, which remain consistent even after processing.

Polyethylene (PE) [$(C_2H_4)_n$] is one of the most massively produced polymers by means of addition polymerization of ethene (C_2H_4). It has a crystalline structure, good mechanical and chemical properties (inertness), and a low price, which makes it ideal for production of packaging ware, construction materials, household items, medical devices, and more [12]. Another very common polymer used in day-to-day life is polyethylene terephthalate (PET). It has similar properties to PE, however, higher strength, and chemical stability [13]. PET is a copolymer made as a result of a polycondensation reaction between ethylene glycol [$(CH_2OH)_2$] and terephthalic acid [$C_6H_4(CO_2H)_2$]. The hydroxyl groups of the ethylene glycol combine with the carboxyl groups of the acid, forming ester (CO-O), which serves as a chemical link. As a by-product of the reaction water is dispersed. PET is typically used for manufacturing of drive belts, conveyor belts, reinforced hoses, high-pressure bottles, etc. Apart from the already mentioned advantages of PET compared to PE, another one can be added – namely its' better recyclability (easier processing) [14].

With the advances in additive manufacturing the requirement for more advanced polymeric materials was imposed. Obviously PET was a great candidate for implementation in such modern methods for production, however, it has one primary drawback – high brittleness. In order to overcome this issue a glycol modifier, particularly 1.4-cyclohexanedimethanol (CHDM) ($C_8H_{16}O_2$) was added to PET, and as a result one of the most popular 3D printing polymers was made – polyethylene terephthalate glycol (PETG) [$(C_{10}H_2O_4)n(C_8H_{16}O_2)m$]. It has an amorphous structure, a higher softening temperature, lower melting temperature, and most importantly much better plasticity compared to PET. Combined with the already excellent functional properties of PET, this material has found incredible application in the field of polymeric additive manufacturing [15].

The possibility of 3D manufacturing of PETG components has already been investigated by previous researchers. Irshadullah et al. [16] have studied and determined the appropriate technological conditions for the manufacturing of PETG molds used for the production of glass, carbon, and Kevlar fiber structures. The authors of [17] have investigated the potential application of PETG printed parts in the field of drone manufacturing. They also investigated different types of thermal treatments on the resultant mechanical properties of the printed samples. Their research points out the positive effect of annealing the samples in salt where a maximal tensile strength of 44.66 MPa was obtained. Iacob et al. [18] have investigated the technical-economical aspect of manufacturing PETG components using the FFF technology, and in all cases obtained samples with a tensile strength between 15 MPa – 30 MPa. Using a 100 % infill density the authors of [19] have managed to obtained a maximum of 79.2 MPa of ultimate tensile strength and 66.9 MPa of flexural strength of PETG samples produced using the FFF technique. A very intriguing method for the recycling and re-using of PETG material was introduced by Dohan et al. [20] who have manufactured a PETG filament entirely based on reused material and compared the mechanical properties of the as-delivered product to the one obtained experimentally. They proved that there was no major difference in the tensile strength of the two filaments as a function of their re-manufacturing. Experimental investigations have also been performed where the mechanical response of PETG manufactured specimens using different infill patterns was determined. In all cases, the results are less than satisfactory with the samples achieving a maximum tensile strength in the range of 10-15 MPa [21]. Previous investigations on the influence of the infill density on the tensile properties of 3D printed PETG components was performed by the authors of [22] with a layer thickness of 0.1 mm. The measured tensile strength was in the range between 17 MPa and 32 MPa. Regardless of the current advances in the knowledge about the fused filament fabrication of PETG components, more data is to be obtained and the correlation between the technological conditions of printing, and the structure, and mechanical properties needs to be further clarified.

Due to this, in the present work PETG samples were printed by means of fused filament fabrication using three different types of infill densities and three different types of patterns. The tensile strength and the flexural strength were determined and an insight on the effect of the infill density and infill patterns on these properties was brought.

2. EXPERIMENTAL PART

The experiments are performed using the fused filament fabrication (FFF) technique as shown in Fig. 1. The polymeric filament is fed into the extrusion head, which consists of a filament feeder and a heated extrusion nozzle. The filament feeder is a system of rollers that mechanically inject the filament into the heated nozzle. The last is preheated to a specified temperature in order to melt the polymer and extrude a single strand of it through the narrowing opening of the nozzle. The extrusion head has

three degrees of movement along the x, y, and z axis. The molten material is deposited on the substrate in a densely viscous liquid form, after which a cooling process occurs. The FFF method is described in detail by the authors of [23]. The 3D model of the desired parts is prepared in advance in Solid Works, then converted to a G-code file, and lastly implemented into the printer software.

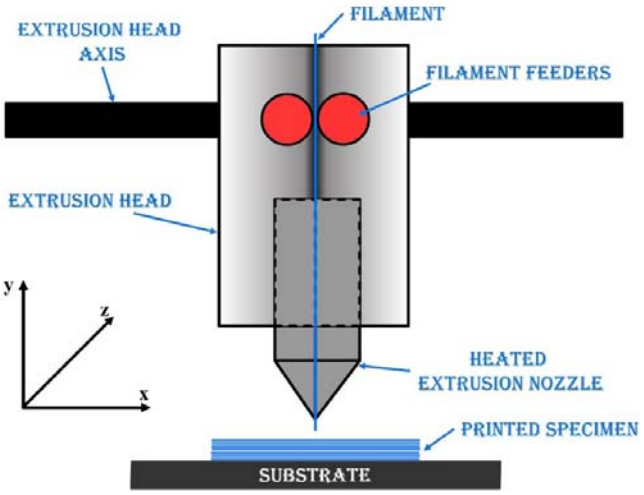

Fig. 1. Schematic of the fused filament fabrication (FFF) process

The filament of chose for the current work is as-delivered polyethylene terephthalate glycol (PETG). The manufacturer's specifications, printing recommendations and cost per gram of material are summarized in table 1. The filament has a diameter of 1.75 mm, and a density of 1.23 g/cm^3. The recommended nozzle temperature by the manufacturer is in the range between 230 ^{o}C and 250 ^{o}C. The recommended bed temperature is between 0 ^{o}C and 80 ^{o}C. The recommended printing speed is in the range between 300 mm/s and 600 mm/s. The price of the filament is 0.02 €/g.

Considering the manufacturer of the PETG filament's recommendations all experiments were carried out using a temperature of the nozzle of 240 ^{o}C, a bed temperature of 80 ^{o}C, and a deposition speed of 300 mm/s. The layer thickness was set to 0.2 mm. The influence of the infill density on the resultant mechanical properties was investigated. For this purpose, the lowest possible densities were chosen, namely 15 %, 25 %, and 35 %. The samples were denoted as T1, T2, and T3, respectively. A standard rectilinear pattern was used. Tensile and flexural tests were then performed and an optimal infill density value was chosen – 35 %.

Subsequently using the selected value, a new set of experiments were performed, where the infill pattern was varied in order to investigate the influence of the different patterns on the mechanical properties of the specimens. Three different patterns were chosen, namely a triangular one, a honeycomb one, and an octet one. The samples were denoted formally as T4, T5, and T6.

Fig. 2 shows the design of all samples. The infill pattern as a function of the infill density of samples T1-T3 can be seen in Figures 2a-c. Figures 2d-f show a view of the selected patterns for samples T4-T6, correspondingly. All technological conditions are summarized in Table 2 along with the necessary print time, total material used per print, and the cost of the material per print.

The dimensions of the tensile samples were selected based on the recommendation of the ISO 527-1:2019 [24] standard for tensile testing of polymeric materials. The as-deposited samples can be seen in Fig. 3a, and the design and dimensions of the samples can be seen in Fig. 3b. The total length of the samples was 170 mm, the length of the test area was 86 mm, the width was 10 mm, and the thickness was 5 mm. Producing the samples to such a size resulted in an area of the testing cross-section of 50 mm^2. In all cases, a ZwickRoell Vibrophore 100 tensile tester was used and set in a static strain mode. The applied pre-load on the samples was 0.1 MPa, and the test speed was 50 mm/min.

The maximum flexural stress of the samples was determined once again using the ZwickRoell Vibrophore 100 unit. The experiment was conducted following the ISO178:2019 [25]. A pre-load of 0.1 MPa was used in all cases with a test speed of 1 mm/min. The test setup is shown in Fig. 4a, and the dimensions of the samples are shown in Fig. 4b. The length of the samples was l=80 mm, the width b=10 mm, and the thickness h=5 mm. The distance between the anvils was L_v=30 mm. The maximum force that the samples can withstand F_{max} [N] was calculated using equation (1) typically used for determining the flexural strength σ_f [MPa] of a 3-point bend test [26].

$$\sigma_f = \frac{3F_{max}L_v}{2bh^2}\,[MPa] \quad (1)$$

An optical microscope Drawell MIT 300/500 was used to investigate the surfaces of the tensile test and flexural test samples. The mechanical response of the samples as a function of the structural response was determined.

Table 2 *Technological conditions of printing, print time, material used, and material cost*

Sample	T_D, °C	T_{BED}, °C	V_D, mm/s	*Print time*	*Material used, g*	*Material cost, €*
T1	*240*	*80*	*300*	*15m42s*	*7.51*	*0.15*
T2	*240*	*80*	*300*	*17m17s*	*8.31*	*0.17*
T3	*240*	*80*	*300*	*18m50s*	*9.11*	*0.18*
T4	*240*	*80*	*300*	*18m48s*	*9.02*	*0.18*
T5	*240*	*80*	*300*	*27m81s*	*9.71*	*0.19*
T6	*240*	*80*	*300*	*24m35s*	*10.34*	*0.21*

Table 1 *Manufacturer's specifications, printing recommendations, and cost of the material*

Manufacturer specifications	***Deposition temperature***	***Print bed temperature***	***Deposition speed***	***Density***	***Diameter***	***Cost***
Value	*230 – 250 °C*	*0 – 80 °C*	*300 – 600 mm/s*	*1.23 g/cm3*	*1.75 mm*	*0.02 €/g*

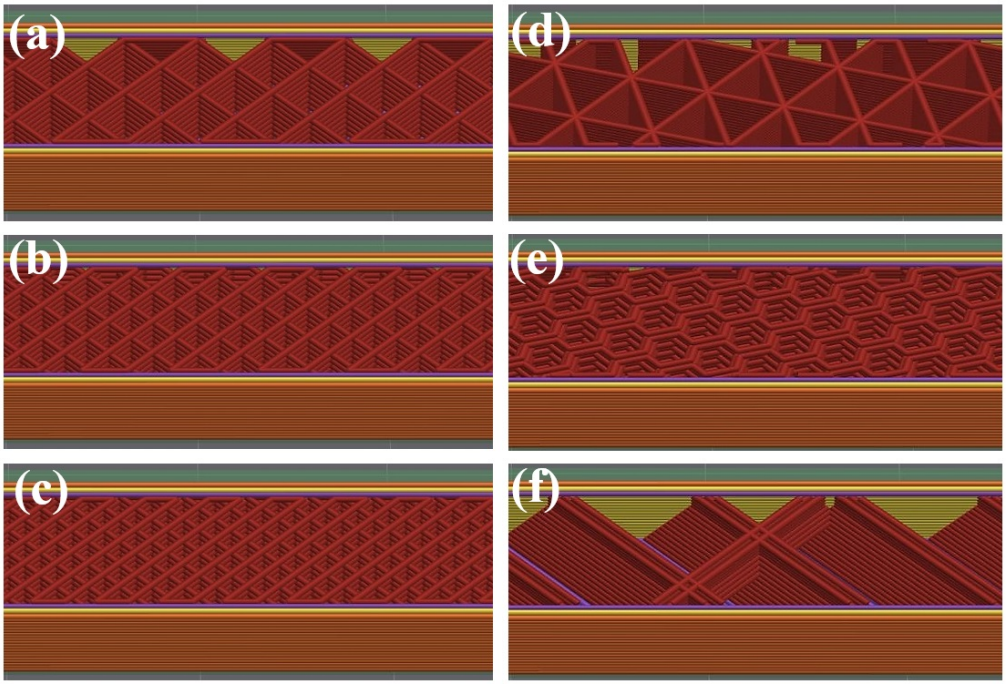

Fig. 2. Infill patterns of samples: a. T1; b. T2; c. T3; d. T4; e. T5; f. T6.

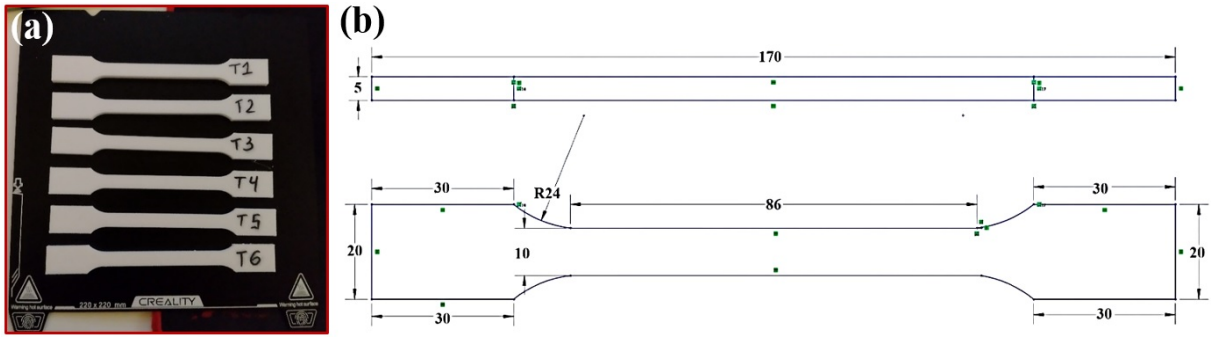

Fig. 3. 3D Printed tensile test samples (a) and sample design and dimensions (b)

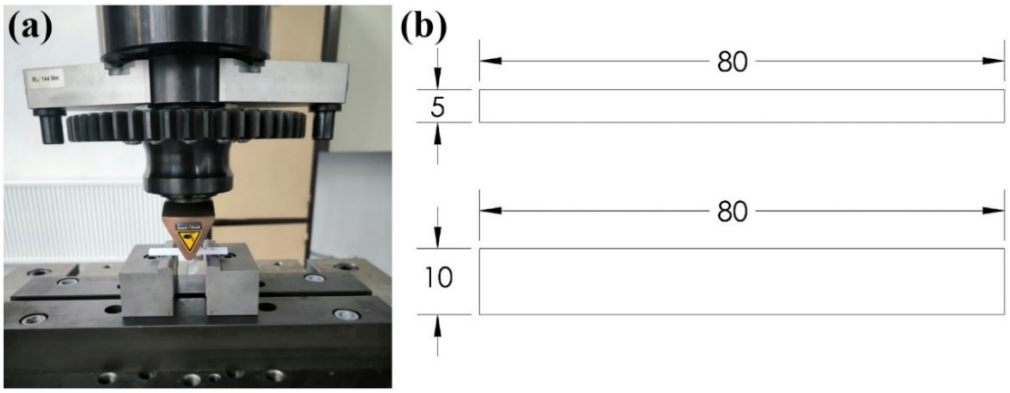

Fig. 4. Flexural test setup (a) and dimensions of the samples (b)

3. RESULTS AND DISCUSSION

In this chapter the tensile test and flexural test results will be presented. All obtained values were summarized in table 3 shown below.

Fig. 5a shows the stress-strain curves and the tensile test results, obtained for samples T1-T3 during the experiments. All curves have a straight sharp slope with a similar incline. In this region, Hooke's law is obeyed, which explains the correlation between the elastic deformation and the applied force. In this instance, all deformation that occurs is purely elastic. Beyond that point, with the increase of the stress the yield point of the material was reached and any further deformation that occurs is purely plastic. The plastic region is very short, meaning that the samples show predominantly an elastic behavior. This hypothesis is confirmed by the measured elongation ε_m [%], which in all cases is about 2 %. The ultimate tensile strength R_m [MPa] of the samples was also determined. Considering specimens T1-T3 with the increase of the infill density the tensile strength slightly increased. The elongation remained approximately the same. The lowest value of the UTS was obtained for the

sample with a 15 % infill – 16.90 MPa, and the highest value was that of sample T3, namely 18.05 MPa.

The flexural test curves for samples T1-T3 can be seen in Fig. 5b. All samples have nearly identical flexural stress-deformation patterns and values with an average flexural strength of 29 MPa. The maximum average force the samples could withstand was about 160 N.

The tensile test fracture zones of samples T1, T2, and T3 are shown in Figures 6a, 6b, and 6c, correspondingly. In all cases, stretching of the infill polymeric strands is observed. As evidenced by the obtained quantitative results sample T3 has the highest tensile strength due to the highest number of individual strands per unit of volume.

Figures 7a, b, and c show the flexural test samples. In the case of sample T1 no major breaking and adhesion problems were observed. In the cases of samples T2 and T3 both adhesion failures between the layers were observed, and substantial failure of individual strands closer towards the bottom of the samples, where the axial tensile forces were the highest.

Table 3 *Tensile and flexural test results of all samples*

Sample	*Tensile tests*		*Flexural tests*		
	R_m, *MPa*	ε_m, *%*	σ_f, *MPa*	ε_f, *%*	F_{max}, *N*
T1 (15%)	*16.90 ±0.51*	*2.01 ±0.11*	*29.0 ±1.21*	*9.2 ±0.46*	*161 ±5*
T2 (25%)	*17.55 ±0.33*	*1.94 ±0.09*	*28.8 ±1.33*	*8.8 ±0.44*	*159 ±4*
T3 (35%)	*18.05 ±0.65*	*1.99 ±0.09*	*29.3 ±1.19*	*8.7 ±0.43*	*163 ±6*
T4 (triangular)	*16.80 ±0.54*	*1.88 ±0.10*	*29.3 ±1.37*	*7.9 ±0.39*	*163 ±4*
T5 (honeycomb)	*18.31 ±0.72*	*1.91 ±0.08*	*31.7 ±1.58*	*8.9 ±0.51*	*176 ±7*
T6 (octet)	*16.16 ±0.44*	*1.65 ±0.09*	*32.4 ±1.61*	*8.9 ±0.53*	*181 ±7*

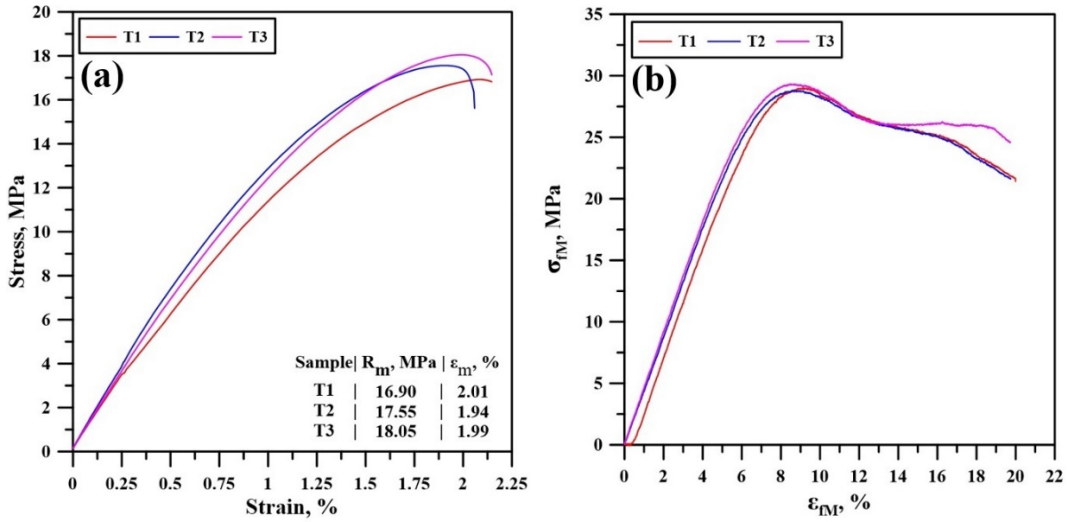

Fig. 5. Stress-strain curves (a) and flexural test curves (b) of samples T1-T3

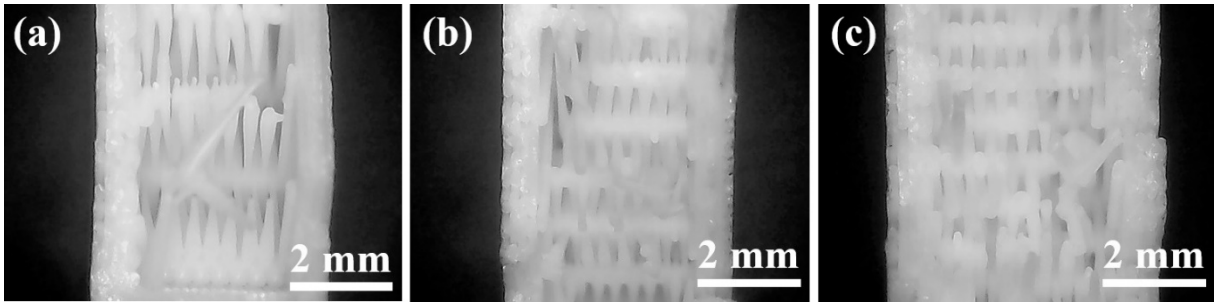

Fig. 6. Fracture zones of (a) sample T1, (b) sample T2, and (c) sample T3

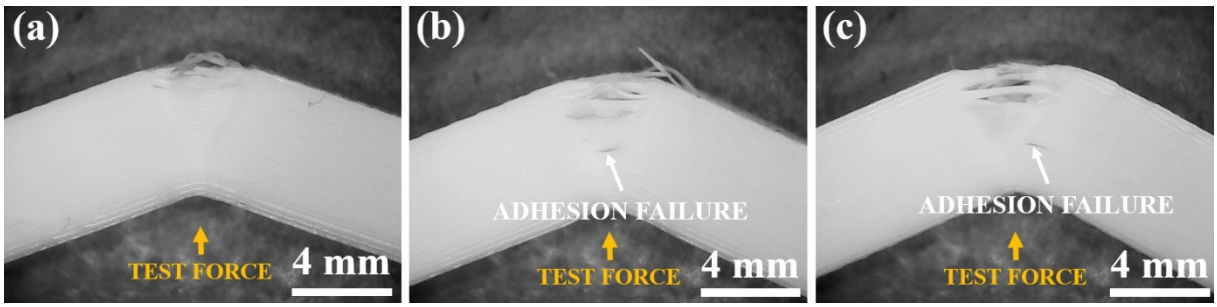

Fig. 7. Flexural test zones of (a) sample T1, (b) sample T2, and (c) sample T3

Figure 8a shows the obtained stress-strain curved for samples T4-T6. In this case a very short plastic region was also noticed, indicating that the samples had predominantly an elastic character. The lowest tensile strength achieved is that of the octet filled sample – 16.16 MPa. This makes sense due to the geometry of the infill, which predominantly consists of triangles positioned next to each other. The specimens are the thinnest at the base of the formed triangles and this is where the fracture occurs. The second highest tensile strength is that of the specimen filled with a triangular infill pattern – 16.80 MPa, and the highest was that of the honeycomb filled sample – 18.31 MPa. This is in agreement with the architecture of the samples, since the honeycomb structure allows for the highest number of joints between the infill of the sample, thus the highest real test area. The fracture zones of samples T4, T5, and T6 are shown in Figures 9a, b, and c, accordingly. In the case of sample T4, the breaking of the sample occurred at the zone where the real cross-section of the sample was the lowest, namely near the edges of the triangular-shaped infill pattern. Due to the formed edge the adhesion in that zone was also the lowest, which propagated the initiation of cracks. Studying specimen T5 a denser structure was formed, along with a high quantity of strands per unit of volume, which improved adhesion. In the case of sample T6, the zone of breaking was where the real cross-section was the thinnest – at the bottom edge of the infill pyramid-like structures. No substantial damage or tearing of the pyramid-shaped infill was observed. Most of the stress was translated to and absorbed by the thin edge of the pyramid and the outer edge of the sample.

Figure 8b shows the results of the flexural tests. Unlike with the infill density in this case an obvious difference between the values can be seen. The lowest flexural strength had the sample prepared with the triangular infill – 29.3 MPa, and the highest was that of the octet filled sample – 32.4 MPa. Figures 10a, b, and c show optical images of samples T4, T5, and T6, correspondingly, after the performed flexural test. It is obvious, substantiated by previous research [27], that during bending the surface of the sample in contact with the indenter is subjected to compressive stress, and the bottom of the sample is subjected to tensile stress. As a result, the initial layers of the samples are in all cases bend. In the cases of samples T4 and T5 which had the triangular and the honeycomb infill patterns the layers towards the bottom of the samples are torn. Adhesion failures at the border between the different layers was also noticed in all cases. However, in the case of the octet filled sample (T6) no breaking of the layers was observed. The layers began to tear at the border between the test zone and the rest of the sample. The most probable reason for this is the geometry of the infill itself. As mentioned previously the octet samples have a triangular infill, which creates a thin weak spot when subjected to a standard axial tensile force. However, it is exactly these triangular shapes that created a support for the samples, as a result of which not only had sample T6 had the highest flexural strength, but also was also damaged the least. As evident from the results layer adhesion is quite the concern since in all cases it was insufficient which has definitely affected the flexural strength of the samples. In this case the questionable adhesion did not affect the tensile strength of neither of the studied samples, however, depending on the printing design this could be a serious issue in the future. More work is necessary in order to improve the adhesion between the layers. Future research is also advisable regarding different infill patterns and designs that would maybe improve the functional properties of the printed samples.

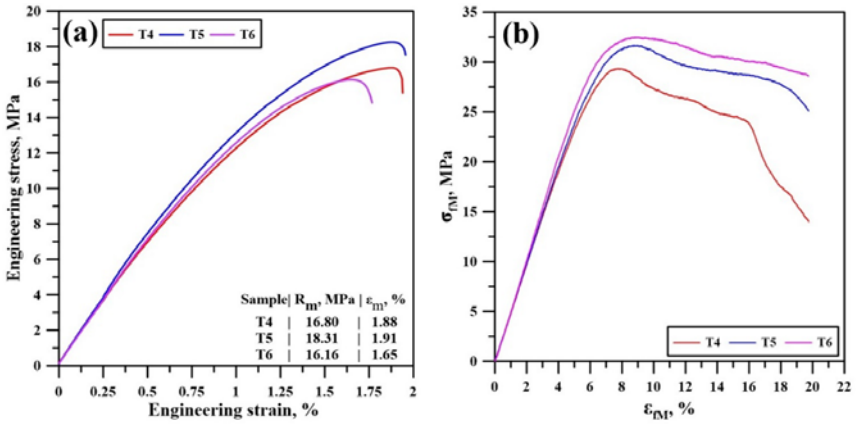

Fig. 8. Stress-strain curves (a) and flexural test curves (b) of samples T4-T6

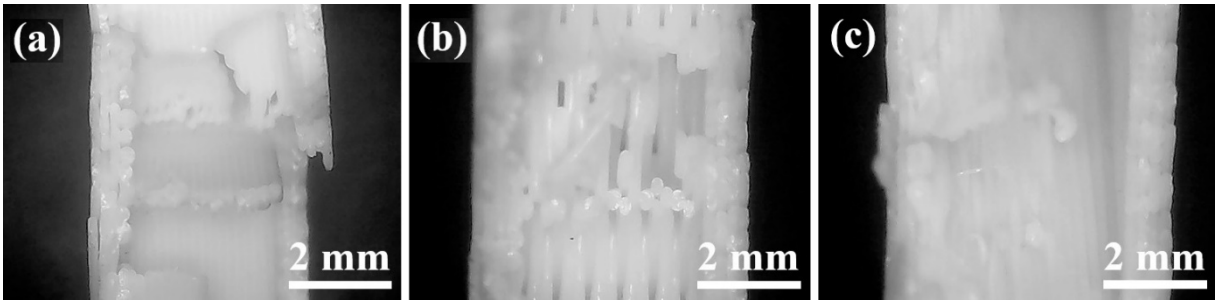

Fig. 9. Fracture zones of (a) sample T4, (b) sample T5, and (c) sample T6

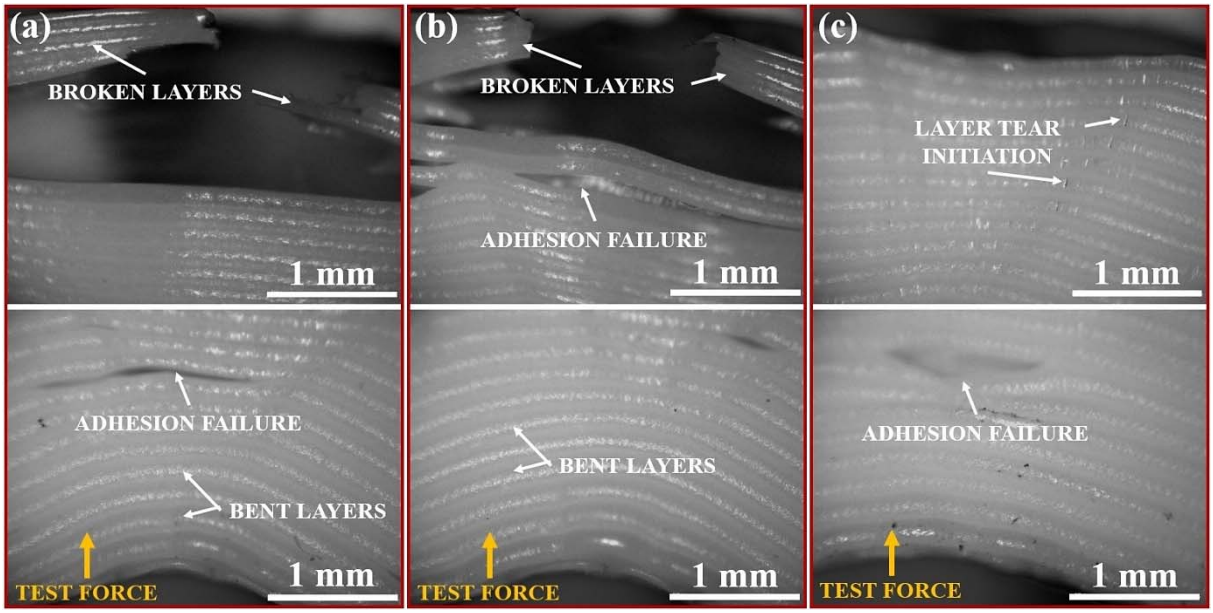

Fig. 10. Flexural test fracture zones of samples: (a) T4; (b) T5, and (c) T6

Comparatively the authors of [28] have studied the influence of the orientation of the infill pattern on the tensile strength of PETG samples. In all cases they obtained values of the last between 40 MPa and 50 MPa, however, they used a 100 % infill pattern. The low values of the tensile strength can be attributed predominantly to the infill density, as confirmed by Durgashyam et al. [29] who have varied the infill density between 60 % and 80 %. The tensile strength of the specimens they prepared varied between 20 MPa and 30 MPa, which is closer to the values obtained in the present work. Previous research has been performed and the studied honeycomb infill structure was proven to have higher compression stress capabilities [30]. The tensile strength was also elevated with the highest value being obtained by employing a 100 % infill density and building the specimen in the vertical direction [30]. A much higher flexural strength of the samples in the range of 60-80 MPa was achieved by the authors of [29], however this could largely be caused by the much higher infill density (in all cases above 60 %). Additionally, the layer thickness and the feed rate were varied. Lower values of the latter were used compared to the ones used in this work and as a result the best mechanical properties were obtained. This is most likely attributed to the smaller footprint of the layer which necessitates less energy in order to adhere and bond with the previously applied layer, which improves the deposition process. Furthermore, a higher deposition resolution is achieved this way, which also seems like an interesting prosper for the further development of the FFF method for manufacturing polymeric components, in this case PETG [31].

Considering the presented results, even though a slight increase in the tensile strength of samples T1-T3 was observed a blatant conclusion can be made that the increase of the infill density in this particular case did not affect the tensile properties of the specimens too much. The same can be said for the flexural strength which remained practically the same. Instead of the infill density, a more major influence had the infill architecture of the samples. The last has to be very well designed and specified in order to meet the strength criteria for the necessary application. In the case of using the samples in such a manner that more tensile force is applied to them a honeycomb pattern is suggested, however, if the printed components are subjected to more flexural stresses an octet infill pattern is preferable.

4. CONCLUSIONS

In agreement with the presented work the following list of conclusions was made:

1. Increasing the infill density from 15 % to 35 % ever so slightly increased the tensile strength of the samples;
2. The infill density did not have an effect on the flexural strength and in all cases it was about 29 MPa;
3. Applying a honeycomb infill pattern resulted in an increased tensile strength, but not an increased flexural strength;
4. Applying an octet infill pattern resulted in the lowest value of the tensile strength of 16.16 MPa, and the highest flexural strength of 32.4 MPa;
5. Bending the samples revealed poor adhesion between parts of the layers;
6. Printing both the honeycomb and the octet samples required more type and input material (thus higher cost of material), however, an improvement of the mechanical properties of the samples was indeed observed, which is not that substantial in these small-scale experiments, but could matter when large-scale 3D parts are produced.

More is to be desired from the mechanical properties of 3D printed PETG components. The present indicates that future research into the specifics of deposition, particularly higher printing resolution and higher infill densities is required. Also finding a good optimal solution for an infill pattern remains as a task, such that would have superb mechanical properties not just regarding a single mechanical test, but all of them combined.

REFERENCES

[1] Kanishka K., Acherjee B., Revolutionizing manufacturing: A comprehensive overview of additive manufacturing processes, materials, developments, and challenges, Journal of Manufacturing Processes 107 (2023) 574-619

[2] Alghamdi S., John S., Choudhury N., Dutta N., Additive Manufacturing of Polymer Materials: Progress, Promise and Challenges, Polymers 13 (2021) 753

[3] Vadafar A., Guzzomi F., Rassau A., Hayward K. Advances in Metal Additive Manufacturing: A Review of Common Processes, Industrial Applications, and Current Challenges, Applied Sciences 11 (2021) 1213

[4] Santos J., Lauers J., Marques A., Maziero R., Galdino A., Influence of 3D printing parameters on the mechanical properties of PETG parts manufactured by FFF, Ibero-American Journal of Polymers 25 (2024) 184-194

[5] Baekeland L., The Synthesis, Constitution, and Uses of Bakelite, Journal of Industrial & Engineering Chemistry, 1 (1909) 149-161

[6] Gee G., The Physical Chemistry of Rubber Solutions, Rubber Chemistry and Technology 17 (1944) 653-678

[7] Gee G., The Molecular Weights of Rubber and Related Materials V, The Interpretation of Molecular Weight Measurements on High Polymers, Rubber Chemistry and Technology 18 (1945) 1-7

[8] Kemp A., Peters H., Fractionation and Molecular Weight of Rubber and Gutta-Percha, Rubber Chemistry and Technology 15 (1942) 1-16

[9] Flory P., Kinetics of Polyesterification: A Study of the Effects of Molecular Weight and Viscosity on Reaction Rate, Journal of the American Chemical Society 12 (1939) 3334-3340

[10] Tadokoro H., Structure and properties of crystalline polymers, Polymer 25 (1984) 147-164

[11] Wendorff J., The structure of amorphous polymers, Polymer 23 (1982) 543-557

[12] Chen L., Lin Z., Polyethylene: Properties, Production and Applications, 2021 3rd International Academic Exchange Conference on Science and Technology Innovation (IAECST), Guangzhou, China (2021) 1191-1196

[13] Sarda P., Hanan J., Lawrence J., Allahkarami M., Sustainability performance of polyethylene terephthalate, clarifying challenges and opportunities, Journal of Polymer Science 60 (2021) 7-31

[14] Suhaimi N., Muhamad F., Razak N., Zeimaran E., Recycling of polyethylene terephthalate wastes: A review of technologies, routes, and applications, Polymer Engineering & Science 62 (2022) 2355-2375

[15] Valvez S., Silva A., Reis P., Compressive Behaviour of 3D-Printed PETG Components, Aerospace 9 (2022) 124

[16] Irshadullah Wasif M., Ftima A., Tufail M., Accurate additively manufactured PETG molds for the composite manufacturing, Proceedings of Researchfora International Conference, Istanbul, Turkey (2023) 6-8

[17] Baltic M., Vasic M., Vorkapic M., Bajic D., Pitel J., Svoboda P., Vencl A., PETG as an Alternative Material for the Production of Drone Spare Parts, Polymers 16 (2024) 2976

[18] Iacob D., Zisopol D., Minescu M., Technical-Economical Study on the Optimization of FDM Parameters for the Manufacture of PETG and ASA Parts, Polymers 16 (2024) 2260

[19] Valvez S., Silva A., Reis P., Optimization of Printing to Maximize the Mechanical Properties of 3D-Printed PETG-Based Parts, Polymers 14 (2022) 2564

[20] Dohan V., Galatanu S., Marsavina L., Mechanical evaluation of recycled PETG filament for 3D printing, Fracture and Structural Integrity 70 (2024) 310-321

[21] Kadhum A., Al-Zubaidi S., Abdulkareem S., Effect of the Infill Patterns on the Mechanical and Surface Characteristics of 3D Printing of PLA, PLA+ and PETG Materials, ChemEngineering 7 (2023) 46

[22] Srinivasan R., Ruban W., Deepanraj A., Bhuvanesh R., Bhuvanesh T., Effect on infill density on mechanical properties of PETG part fabricated by fused deposition modeling, Materials Today: Proceedings 27 (2020) 1838-1842

[23] Rashid A., Koc M., Fused Filament Fabrication Process: A Review of Numerical Simulation Techniques, Polymers 13 (2021) 3534

[24] ISO527-1:2019 Plastics – Determination of tensile properties. ISO: Geneva, Switzerland, 2019

[25] ISO178:2019 Plastics – Determination of flexural properties. ISO: Geneva, Switzerland, 2019

[26] Junior S., Ferracane J., Bona A., Flexural strength and Weibull analysis of a microhybrid and a nanofill composite evaluated by 3- and 4-point bending tests, Dental Materials 24 (2008) 426-431

[27] Tuncel O., Kahya C., Tufekci K., Optimization of Flexural Performance of PETG Samples Produced by Fused Filament Fabrication with Response Surface Method, Polymers 16 (2024) 2020

[28] Dolzyk G., Jung S., Tensile and Fatigue Analysis of 3D-Printed Polyethylene Terephthalate Glycol, Journal of Failure Analysis and Prevention 19 (2019) 511-518

[29] Durgashyam K., Reddy M., Balakrishna A., Satyanarayana K., Experimental investigation on mechanical properties of PETG material processed by fused deposition modeling method, Materials Today: Proceedings 18 (2019) 2052-2059

[30] Basurto-Vazquez O., Sanchez-Rodriguez E., McShane G., Medina D., Load Distribution on PET-G 3D Prints of Honeycomb Cellular Structures under Compression Load, Polymers 13 (2021) 1983

[31] Shergill K., Chen Y., Bull S., What controls layer thickness effects on the mechanical properties of additive manufactured polymers, Surface & Coatings Technology 475 (2023) 130131